Dynamic Modeling of a Full Toroidal Variator: the Power-Oriented Graphs approach

Roberto Zanasi, Federica Grossi and Marco Fei

***Abstract*— The Full Toroidal Variator is the core element in many mechanical hybrid systems for vehicle applications like Kinetic Energy Recovery System and Infinitely Variable Transmission because it allows to manage the power transfer with continuous variation of the speed-ratio.**

In this paper the model of a Full Toroidal Variator is addressed using Power-Oriented Graphs (POG) that is an energy-based modeling technique. Modeling with POG allows to easily transform and reduce the model when some dynamics of the system go to zero. An extended and reduced POG model of the Full Toroidal Variator are given. Simulation results of the modeled system are shown.

I. INTRODUCTION

For modeling complex dynamic physical systems the exploitation of a modeling technique supported by theoretical bases is very important. The concept of energy moving within the system is at the basis of the so called energy-based modeling techniques, many of which have been introduced in the past years: the Bond Graphs (BG) [1], [2], the Power-Oriented Graphs (POG) [3] and the Energetic Macroscopic Representation (EMR) [4]. Some comparisons among these techniques can be found in [5] and [6].

In this paper the modeling of a Full Toroidal Variator (FTV) is addressed using the POG approach. The FTV, see [7], [8] and [9], is the key element in vehicle applications as Kinetic Energy Recovery System (KERS) and Infinitely Variable Transmission (IVT) because it allows power transfer with continuous variation of the speed-ratio. The main advantages of using the POG technique are: POG block schemes are easy to draw and can be understood even by beginners; the power sections and the power flows within the system are clearly shown; the dissipative behavior of the model is guaranteed; the equations of the model are represented by a POG block scheme which is in direct correspondence with state space equations; some congruent state space transformations can be used to transform and reduce the model, preserving the system properties, when some dynamics go to zero, see [10]; the POG scheme can be directly translated into Simulink; the modular structure based on power sections allows to build the whole model by composing subsystems models.

II. POWER-ORIENTED GRAPHS (POG) BASIC CONCEPTS

The POG block schemes [3] are standard block diagrams combined with a particular modular structure essentially based on the use of two blocks: the *elaboration block* (e.b.) and the *connection block* (c.b.). The e.b., shown in Fig. 1.a describes all the physical elements that stores and/or dissipates energy (i.e. springs, masses, dampers, capacitors, inductors, resistors, etc.). The circle in the e.b. is a summation element and the black spot represents a minus sign that multiplies the entering variable. The c.b., shown in Fig. 1.b, describes all the physical elements that redistributes the power within the system without storing nor dissipating energy (i.e. any type of gear reduction, transformers, etc.). The c.b. transforms the power variables satisfying the constraint $\mathbf{x}_1^{\mathrm{T}}\mathbf{y}_1 = \mathbf{x}_2^{\mathrm{T}}\mathbf{y}_2$. The e.b. and the c.b. are suitable for representing both scalar and vectorial systems. In the vectorial case $\mathbf{G}(s)$ and $\mathbf{K}$ are matrices: $\mathbf{G}(s)$ is always a square matrix composed by positive real transfer functions and $\mathbf{K}$ can be rectangular and time-varying. The main feature of the POG is to keep a direct correspondence between the dashed sections of the graphs and the real power sections of the modeled physical systems: the scalar product $\mathbf{x}^{\mathrm{T}}\mathbf{y}$ of the two *power variables* $\mathbf{x}$ and $\mathbf{y}$ involved in each dashed line of a POG, see Fig. 1, has the physical meaning of *power flowing through the section*.

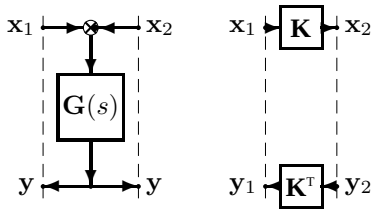

a) *e. b.* b) *c. b.*

Fig. 1. POG basic blocks: a) *elaboration block*; b) *connection block*.

A. POG state space dynamic models

The POG schemes are in direct correspondence with state space dynamic equations of the system. For example, the

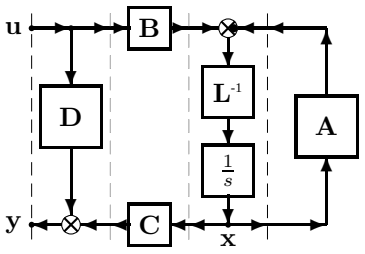

$$\begin{cases} \mathbf{L}\,\dot{\mathbf{x}} = -\mathbf{A}\,\mathbf{x} + \mathbf{B}\,\mathbf{u} \\ \mathbf{y} = \mathbf{C}\,\mathbf{x} + \mathbf{D}\,\mathbf{u} \end{cases} \quad (1)$$

$$\Downarrow (\mathbf{x} = \mathbf{T}\,\mathbf{z})$$

$$\begin{cases} \overline{\mathbf{L}}\,\dot{\mathbf{z}} = -\overline{\mathbf{A}}\,\mathbf{z} + \overline{\mathbf{B}}\,\mathbf{u} \\ \mathbf{y} = \overline{\mathbf{C}}\,\mathbf{z} + \overline{\mathbf{D}}\,\mathbf{u} \end{cases} \quad (2)$$

Fig. 2. POG block scheme of a generic dynamic system.

Roberto Zanasi, Federica Grossi and Marco Fei are with the Department of Engineering "Enzo Ferrari", University of Modena and Reggio Emilia, Modena, Italy {roberto.zanasi, federica.grossi, marco.fei}@unimore.it.

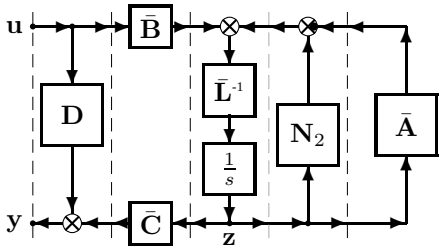

Fig. 3. POG block scheme of the transformed dynamic system (3).

POG scheme shown in Fig. 2 can be represented by the state space equations (1) where $\mathbf{x} \in \mathbb{R}^n$ is the state vector, $\mathbf{u} \in \mathbb{R}^m$ is the input and $\mathbf{y} \in \mathbb{R}^m$ is the output. The *energy matrix* $\mathbf{L}$ is always symmetric and positive definite: $\mathbf{L} = \mathbf{L}^{\mathrm{T}} > 0$. The POG form (1) is similar to the notations used for the port-Hamiltonian equations in co-energy variables [11] and in generalized state-space equations [12]. Using a constant "congruent" transformation $\mathbf{x} = \mathbf{T}\mathbf{z}$, where $\mathbf{z} \in \mathbb{R}^p$, $p \leq n$ and $\mathbf{T} \in \mathbb{R}^{n \times p}$, the dynamic model (1) can be transformed into system (2) where: $\overline{\mathbf{L}} = \mathbf{T}^{\mathrm{T}}\mathbf{L}\mathbf{T}$, $\overline{\mathbf{A}} = \mathbf{T}^{\mathrm{T}}\mathbf{A}\mathbf{T}$, $\overline{\mathbf{B}} = \mathbf{T}^{\mathrm{T}}\mathbf{B}$, $\overline{\mathbf{C}} = \mathbf{C}\mathbf{T}$ and $\overline{\mathbf{D}} = \mathbf{D}$.
When matrix $\mathbf{T}$ is time-varying, the transformed matrices $\bar{\mathbf{L}}$, $\bar{\mathbf{A}}$, $\bar{\mathbf{B}}$ and $\bar{\mathbf{C}}$ are time-varying too and an additional term $\mathbf{N}_2\mathbf{z} = -\mathbf{T}^{\mathrm{T}}\mathbf{L}\dot{\mathbf{T}}\mathbf{z}$ appears in the transformed system:

$$\begin{cases} \underbrace{\mathbf{T}^{\mathrm{T}}\mathbf{L}\mathbf{T}}_{\bar{\mathbf{L}}}\,\dot{\mathbf{z}} + \underbrace{\mathbf{T}^{\mathrm{T}}\mathbf{L}\dot{\mathbf{T}}}_{-\mathbf{N}_2}\,\mathbf{z} = -\underbrace{\mathbf{T}^{\mathrm{T}}\mathbf{A}\mathbf{T}}_{\bar{\mathbf{A}}}\,\mathbf{z} + \underbrace{\mathbf{T}^{\mathrm{T}}\mathbf{B}}_{\bar{\mathbf{B}}}\,\mathbf{u} \\ \mathbf{y} = \underbrace{\mathbf{C}\mathbf{T}}_{\bar{\mathbf{C}}}\,\mathbf{z} + \underbrace{\mathbf{D}}_{\bar{\mathbf{D}}}\,\mathbf{u} \end{cases} \tag{3}$$

System (3) can be represented by the POG scheme of Fig. 3: note that block $\mathbf{N}_2$ is structurally connected with the dynamic block $\bar{\mathbf{L}}$, therefore only the two blocks considered together properly describe a time-varying dynamic block. When $\mathbf{L}$ is constant, it can be proved that the symmetric part $\mathbf{N}_{2s}$ of $\mathbf{N}_2$ is

$$\mathbf{N}_{2s} = \frac{\mathbf{N}_2 + \mathbf{N}_2^{\mathrm{T}}}{2} = -\frac{\dot{\mathbf{L}}}{2} \tag{4}$$

When $p = 1$ (i.e. $\mathbf{T}$ is a column matrix) matrices $\bar{\mathbf{L}}$, $\bar{\mathbf{A}}$, $\bar{\mathbf{B}}$, $\bar{\mathbf{C}}$ and $\bar{\mathbf{N}}_2$ degenerate to scalars and from (4) it follows

$$N_2 = -\frac{\dot{L}}{2} \tag{5}$$

When an eigenvalue of matrix $\mathbf{L}$ tends to zero (or to infinity), system (1) degenerates towards a lower dimension dynamic system. In this case the reduced and transformed system can be obtained using a "rectangular" matrix $\mathbf{T}$, see [10].

III. Dynamic Model of a Full Toroidal Variator

The Full Toroidal Variator is the key element in vehicle applications, see [7], [8] and [9]. In KERS applications the FTV manages the power flows between the vehicle and a flywheel (the kinetic energy is stored in the flywheel during braking and then reused under acceleration of the vehicle). In IVT applications the FTV is coupled with an epicyclic gear to allow the control of power flows in the powertrain by a continuous change of the speed-ratio over a wide range. A schematic of the considered FTV is shown in Fig. 4.

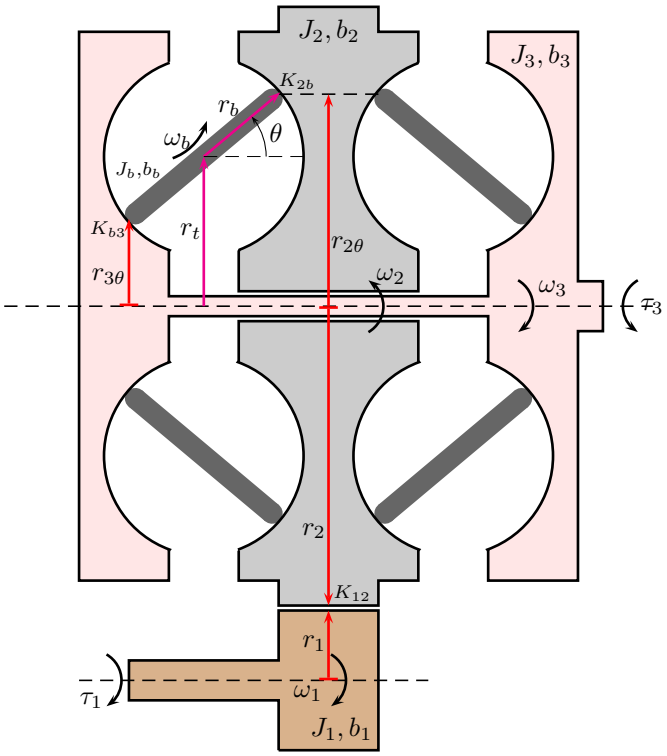

Fig. 4. Schematic of a Full Toroidal Variator.

J_1	shaft moment of inertia
b_1	shaft linear friction coefficient
ω_1	shaft angular velocity
τ_1	torque acting on the shaft
r_1	gear radius
K_{12}	stiffness coefficient between shaft and inner disk
J_2, J_3	inner and outer disks moments of inertia
b_2, b_3	inner and outer disks linear friction coefficients
ω_2, ω_3	inner and outer disks angular velocities
τ_3	torque acting on the outer disk
r_2	inner disk radius
θ	tilt angle of the rollers
$r_{2\theta}$, $r_{3\theta}$	contact radial positions
K_{2b}, K_{3b}	contact stiffness coefficients
J_b	rollers moment of inertia
b_b	rollers linear friction coefficient
ω_b	rollers angular velocity
r_b	rollers radius
r_t	toroid centerline radius

TABLE I
Parameters and variables of the Full Toroidal Variator.

The meaning of parameters and variables of the system is reported in Table I.
The two toroidal cavities contain six rollers (three for each cavity) that transfer the power from the inner disc to the outer disc and viceversa. The variator speed-ratio is a function of the rollers inclination: a change of the tilt angle θ of the rollers causes a speed-ratio variation. The contact radial positions $r_{2\theta}$ and $r_{3\theta}$ are related to radii r_t and r_b as follows:

$$r_{2\theta} = r_t + r_b \sin\theta, \qquad r_{3\theta} = r_t - r_b \sin\theta.$$

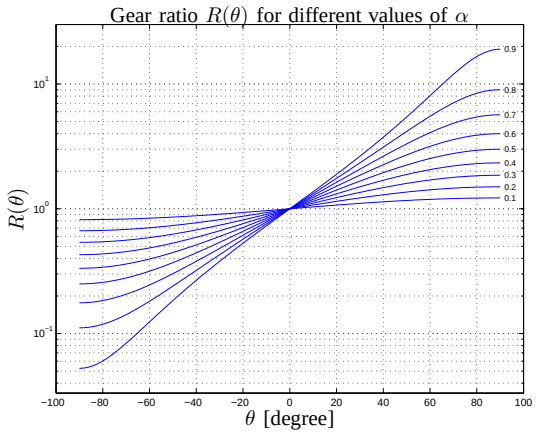

Fig. 5. Gear ratio $R(\theta)$ for different values of $\alpha \in [0.1 : 0.1 : 0.9]$.

The gear ratio $R(\theta)$ relating the angular speed ω_2 of the inner disk to the angular speed ω_3 of the outer disk is function of the tilt angle θ as follows:

$$R(\theta) = \frac{\omega_3}{\omega_2} = \frac{r_{2\theta}}{r_{3\theta}} = \frac{r_t + r_b \sin\theta}{r_t - r_b \sin\theta} = \frac{1 + \alpha \sin\theta}{1 - \alpha \sin\theta} \qquad (6)$$

where $\alpha = \frac{r_b}{r_t}$. A plot of the gear ratio $R(\theta)$ for different values of $\alpha \in [0.1 : 0.1 : 0.9]$ is given in Fig. 5. The FTV is a non-linear and time-variant system and writing its lumped parameter dynamic model can be a non trivial problem: the POG approach makes this task easier. The POG model of a physical system can be obtained in this way: identify the power sections of the system and, following the power flows, draw the POG scheme from left to right putting between each pair of adjacent power sections the POG block of the considered physical element. The POG block scheme of the considered FTV system is shown in Fig. 6. The introduction of fictitious dynamic elements, that can be afterwards eliminated from the model, is useful to simplify the writing down of a dynamic model characterized only by integral causality (mandatory to have a model suitable for simulation). For this reason the gear ratios are here modeled by using "fictitious" elastic elements (i.e. the only dynamic element that can be put between two masses or inertias respecting integral causality) that can be eliminated simplifying the model and obtaining, with the reduction method explained in this section, both the equations of the model without the fictitious elements and the explicit expressions of parameters of the reduced model.

The state space dynamic model of the POG system shown in Fig. 6 is:

$$\mathbf{L}\,\dot{\mathbf{x}} = -\mathbf{A}\,\mathbf{x} + \mathbf{B}\mathbf{u} \qquad (7)$$

where matrices and vectors $\mathbf{L}$, $\mathbf{A}$, $\mathbf{B}$, $\mathbf{x}$, $\mathbf{u}$ are defined as:

$$\mathbf{L} = \begin{bmatrix} J_1 & & & & & & \\ & K_{12}^{-1} & & & & & \\ & & J_2 & & & & \\ & & & K_{2b}^{-1} & & & \\ & & & & J_b & & \\ & & & & & K_{b3}^{-1} & \\ & & & & & & J_3 \end{bmatrix},$$

$$\mathbf{A} = \begin{bmatrix} -b_1 & -r_1 & & & & & \\ r_1 & 0 & -r_2 & & & & \\ & r_2 & -b_2 & -r_{2\theta} & & & \\ & & r_{2\theta} & 0 & -r_b & & \\ & & & r_b & -b_b & -r_b & \\ & & & & r_b & 0 & -r_{3\theta} \\ & & & & & r_{3\theta} & -b_3 \end{bmatrix},$$

$$\mathbf{B} = \begin{bmatrix} 1 & 0 \\ 0 & 0 \\ 0 & 0 \\ 0 & 0 \\ 0 & 0 \\ 0 & 0 \\ 0 & -1 \end{bmatrix}, \quad \mathbf{x} = \begin{bmatrix} \omega_1 \\ f_{12} \\ \omega_2 \\ f_{2b} \\ \omega_b \\ f_{b3} \\ \omega_3 \end{bmatrix}, \quad \mathbf{u} = \begin{bmatrix} \tau_1 \\ \tau_3 \end{bmatrix}.$$

The procedure to write the state space equations from a POG scheme is explained in [14]. When the stiffnesses K_{12}, K_{2b} and K_{b3} tend to infinity, the POG model can be transformed and reduced to a one-dimensional time-varying dynamic system by using a congruent transformation, as stated in Section II-A.

When $K_{12} \to \infty$, $K_{2b} \to \infty$ and $K_{b3} \to \infty$ the state variables are related by the following relations:

$$\begin{aligned} \omega_2 &= \frac{r_1}{r_2}\,\omega_1, \\ \omega_b &= \frac{r_{2\theta}}{r_b}\,\omega_2 = \frac{r_{2\theta}\,r_1}{r_b\,r_2}\,\omega_1, \\ \omega_3 &= \frac{r_b}{r_{3\theta}}\,\omega_b = \frac{r_{2\theta}\,r_1}{r_{3\theta}\,r_2}\,\omega_1. \end{aligned} \qquad (8)$$

The following state space congruent transformation is used:

$$\mathbf{x} = \mathbf{T}(\theta)\,\omega_1 \quad \Leftrightarrow \quad \underbrace{\begin{bmatrix} \omega_1 \\ f_{12} \\ \omega_2 \\ f_{2b} \\ \omega_b \\ f_{b3} \\ \omega_3 \end{bmatrix}}_{\mathbf{x}} = \underbrace{\begin{bmatrix} 1 \\ 0 \\ \frac{r_1}{r_2} \\ 0 \\ \frac{r_1\,r_{2\theta}}{r_2\,r_b} \\ 0 \\ \frac{r_1\,r_{2\theta}}{r_2\,r_{3\theta}} \end{bmatrix}}_{\mathbf{T}(\theta)} \omega_1 = \underbrace{\begin{bmatrix} 1 \\ 0 \\ R_2 \\ 0 \\ R_b(\theta) \\ 0 \\ R_3(\theta) \end{bmatrix}}_{\mathbf{T}(\theta)} \omega_1$$

where gear ratios R_2, $R_b(\theta)$ and $R_3(\theta)$ are the following:

$$R_2 = \frac{r_1}{r_2}, \qquad R_b(\theta) = \frac{r_1\,r_{2\theta}}{r_2\,r_b} = \frac{r_1\,(r_t + r_b \sin\theta)}{r_2\,r_b},$$

$$R_3(\theta) = \frac{r_1\,r_{2\theta}}{r_2\,r_{3\theta}} = \frac{r_1\,(r_t + r_b \sin\theta)}{r_2\,(r_t - r_b \sin\theta)}.$$

Since the transformation matrix $\mathbf{T}(\theta)$ is a column matrix, the transformed and reduced model is a first order dynamic model that can be written in the following *explicit* form:

$$\bar{L}(\theta)\,\dot{\omega}_1 - N_2(\theta, \dot{\theta})\,\omega_1 = -\bar{A}(\theta)\,\omega_1 + \begin{bmatrix} 1 & -R_3(\theta) \end{bmatrix} \begin{bmatrix} \tau_1 \\ \tau_3 \end{bmatrix} \qquad (9)$$

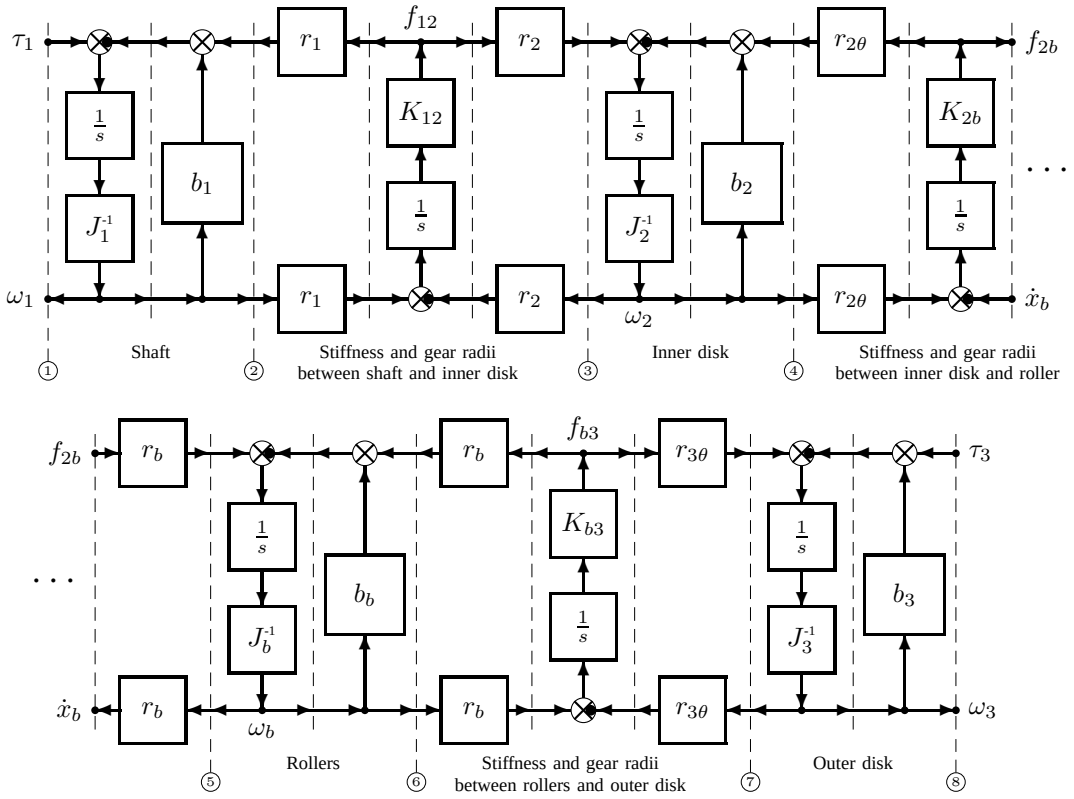

Fig. 6. POG block scheme of the Full Toroidal Variator.

where coefficients $\bar{L}(\theta) = \mathbf{T}^{\mathrm{T}}\mathbf{L}\mathbf{T}$ and $\bar{A}(\theta) = \mathbf{T}^{\mathrm{T}}\mathbf{A}\mathbf{T}$ are:

$$\begin{aligned}\bar{L}(\theta) &= J_1 + R_2^2\, J_2 + R_b^2(\theta)\, J_b + R_3^2(\theta)\, J_3 \\ &= J_1 + \tfrac{r_1^2}{r_2^2}\, J_2 + \tfrac{r_1^2}{r_2^2}\,\tfrac{r_{2\theta}^2}{r_b^2}\, J_b + \tfrac{r_1^2}{r_2^2}\,\tfrac{r_{2\theta}^2}{r_{3\theta}^2}\, J_3 \\ \bar{A}(\theta) &= b_1 + R_2^2\, b_2 + R_b^2(\theta)\, b_b + R_3^2(\theta)\, b_3 \\ &= b_1 + \tfrac{r_1^2}{r_2^2}\, b_2 + \tfrac{r_1^2}{r_2^2}\,\tfrac{r_{2\theta}^2}{r_b^2}\, b_b + \tfrac{r_1^2}{r_2^2}\,\tfrac{r_{2\theta}^2}{r_{3\theta}^2}\, b_3\end{aligned}$$

and coefficient $N_2(\theta, \dot{\theta})$ is obtained applying relation (5):

$$N_2(\theta, \dot{\theta}) = -\frac{\dot{\bar{L}}(\theta)}{2} = -r_{2\theta}\, r_b\, \dot{\theta} \cos\theta\, R_2^2 \left(\frac{J_b}{r_b^2} + \frac{2\, r_t\, J_3}{r_{3\theta}^3} \right).$$

The POG scheme of the transformed and reduced system (9) is shown in Fig. 7. Note that the input and output power sections ① and ⑧ of the POG in Fig. 7 are the same of the POG scheme shown in Fig. 6. Another example of model reduction obtained by using a POG congruent transformation can be found in [10] for a planetary gear. This methodology to reduce model order is somehow similar to the Singular Perturbation approach, see [13], when the dynamics of the additional fictitious elements is assumed to be much faster than the dynamics of the physical elements present in the reduced order system.

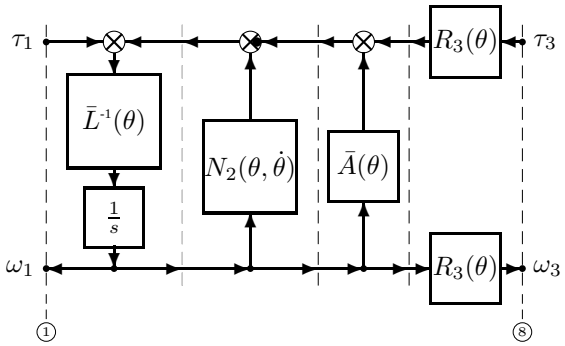

Fig. 7. POG scheme of the transformed and reduced system (9).

A. Torsional dynamics of the rollers

In the FTV the speed ratio defined in (6) is a function of the tilt angle θ. This angle can change in two ways: when the inner/outer disks speeds change, the rollers steer to a new angle θ according to the new speed ratio (self alignment); viceversa the roller tilt angle θ can be set by applying hydraulic pressure causing a variation of the speed ratio and accelerating the inner/outer disks.

Since the focus of the paper is to show the modeling methodology, in this simplified model the self alignment property is neglected. The POG block scheme representing the torsional dynamics of the rollers together with the hydraulic actuation system is shown in Fig. 8.

By modulating the external pressure P_r a volume flow rate Q_r enters into the hydraulic capacity C_t generating a pressure P_t within the mechanical circuit that makes the roller tilt. Pressure P_t, multiplied by h_t, generates the torque τ_t acting on the inertia J_t of the rollers. The parameter h_t

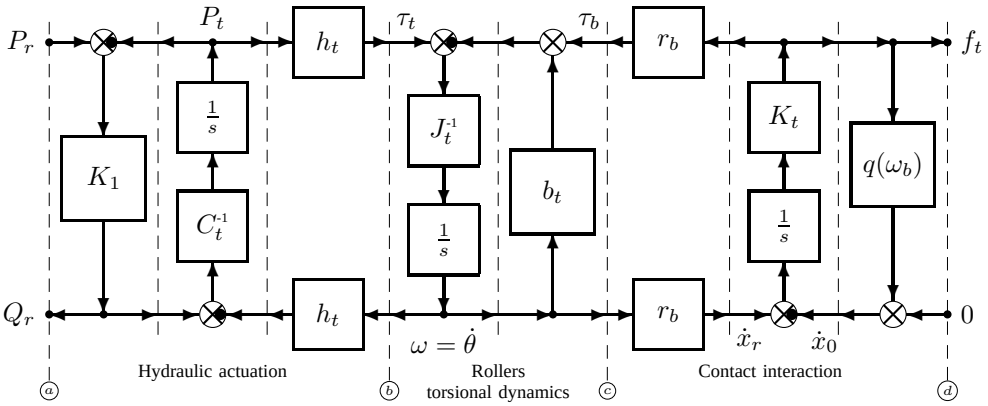

Fig. 8. POG block scheme of the hydraulic actuation and torsional dynamics of the rollers.

is a proper "angular area" that describes the effect of the castor angle. A first reaction torque acting on the inertia J_t is given by the torsional friction b_t. A further reaction torque τ_b is generated at the contact point between the rollers and the disks. This contact interaction is modeled by an elastic element, see Fig. 9, characterized by the lumped stiffness K_t that generates the load force f_t that, multiplied by the roller radius r_b, gives the torque τ_b. The elastic element K_t has two terminals: x_r on the roller and x_0 moving on the disk. The velocity of the second terminal $\dot{x}_0$ is expressed by relation $\dot{x}_0 = q(\omega_b)\, f_t$ where $q(\omega_b)$ is a function (even nonlinear) of the angular speed ω_b of the rollers. This model takes into account that if the rollers are not rotating, i.e. $\omega_b = 0$, then the requested torque to tilt the roller must be very high. In normal operating mode the roller tilt angle θ is changed only when the roller angular speed is different from zero.

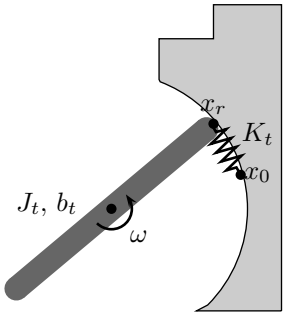

Fig. 9. Elastic interaction between the rollers and the disk.

IV. Simulation

The two POG models shown in Fig. 7 and Fig. 8 have been implemented in Matlab using the Simulink model shown in Fig. 10. The Simulink schemes of the two subsystems "Full Toroidal Variator" and "Rollers" are shown in Fig. 11 and Fig. 12, respectively. Note that there is a direct correspondence between the POG models and Simulink schemes. A position control on the angular position θ has been implemented by using a proportional controller K_p. The control pressure P_r is saturated to a maximum value $P_{max} = \pm 40$ bar. The input torques are zero $\tau_1 = \tau_3 = 0$ Nm and the reference tilt

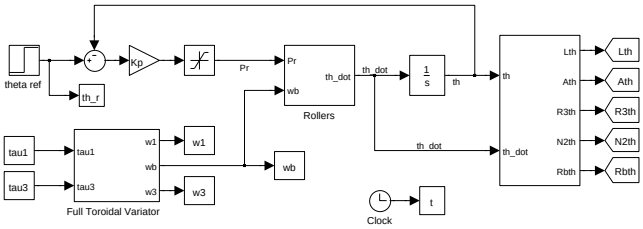

Fig. 10. Simulink scheme of the position controlled Full Toroidal Variator.

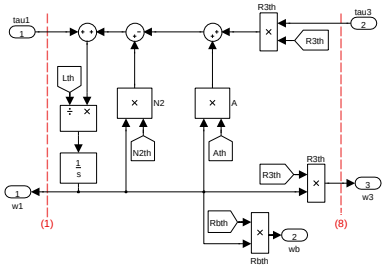

Fig. 11. Simulink scheme of the subsystem "Full Toroidal Variator".

angle θ is changed from $15°$ to $-25°$ at the time $t = 0.03$ s.

The main parameters used in simulation are shown in Table II. The tilt angle $\theta(t)$, the angular speed of the rollers $\omega(t)$ and pressures $P_t(t)$ and $P_r(t)$ are shown in Fig. 13. The oscillation of the tilt angle $\theta(t)$ is caused by both the elastic contact interaction of the rollers and the control. The angular speeds ω_1 (the shaft), ω_b (the roller) and ω_3 (the outer disks) are shown in Fig. 14. The gear ratios $R(\theta)$,

TABLE II
Main parameters of the system

J_1	260	kg cm^2
J_2	18	kg cm^2
J_3	18	kg cm^2
J_b	1.7	kg cm^2
J_t	10	kg cm^2
r_1	17.2	mm
r_2	51.5	mm
r_b	27.5	mm
r_t	34.3	mm

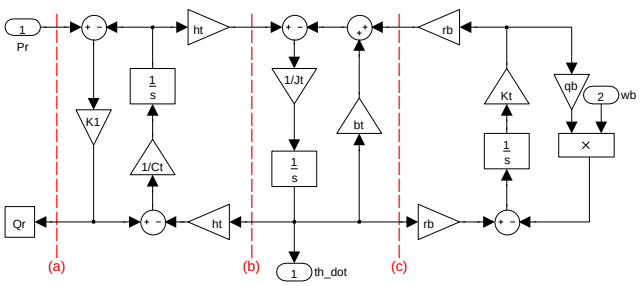

Fig. 12. Simulink scheme of the subsystem "Roller".

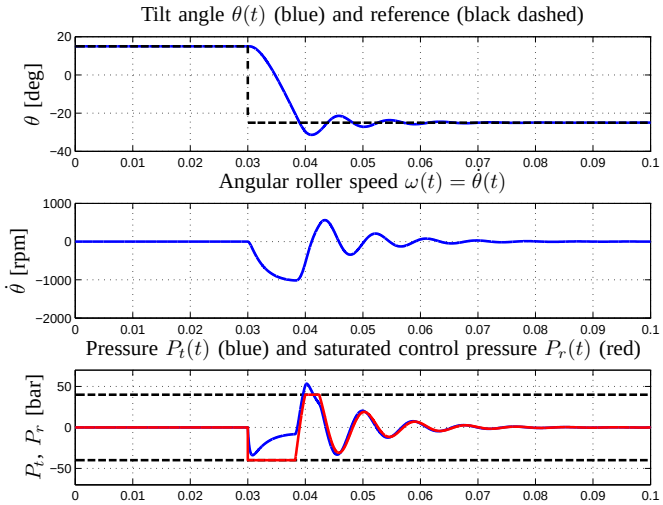

Fig. 13. Tilt angle $\theta(t)$, angular speed of the rollers $\omega(t)$ and pressures $P_t(t)$ and $P_r(t)$.

R_{12}, $R_b(\theta)$ and $R_3(\theta)$ are shown in Fig. 15. Note that the dashed line represents the theoretical $R(\theta)$ and the portion of the curve in red solid line is the one obtained in simulation.

V. CONCLUSION

The Power-Oriented Graphs (POG) energy-based modeling technique is here exploited to model a Full Toroidal Variator. Taking advantages from the POG property of transforming and reducing dynamic systems, both an extended and reduced model for the Full Toroidal Variator have been given. Also the modeling of torsional dynamics of the rollers has been addressed. Some Simulink simulations of the modeled system with a simple control of the roller tilt angle have been reported, showing the effectiveness of the proposed model.

REFERENCES

[1] H.M. Paynter, *Analysis and Design of Engineering Systems*, MIT-press, Camb., MA, 1961.

[2] D. C. Karnopp, D.L. Margolis, R. C. Rosemberg, *System dynamics - Modeling and Simulation of Mechatronic Systems*, Wiley Interscience, ISBN 0-471-33301-8, 3rd ed. 2000.

[3] R.Zanasi, "The Power-Oriented Graphs technique: System modeling and basic properties", Proceeding of 2010 IEEE Vehicle Power and Propulsion Conference (VPPC), 2010, pp.1-6

[4] J. C. Mercieca, J. N. Verhille, A. Bouscayrol, "Energetic Macroscopic Representation of a subway traction system for a simulation model", Proceeding of IEEE-ISIE 2004, May 2004, pp.1519-1524

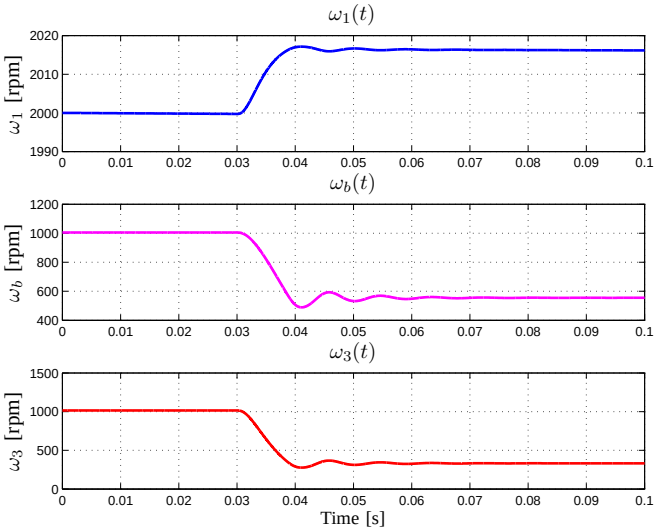

Fig. 14. Angular speed ω_1 of the shaft, ω_b of the roller and ω_3 of outer disks.

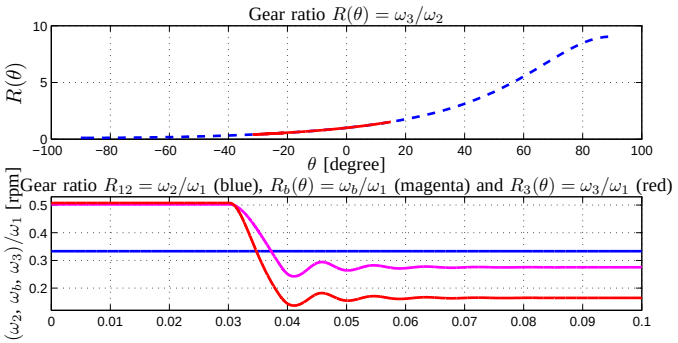

Fig. 15. Gear ratios: $R(\theta)$, R_{12}, $R_b(\theta)$ and $R_3(\theta)$.

[5] R. Zanasi, G. H. Geitner, A. Bouscayrol, W. Lhomme, "Different energetic techniques for modelling traction drives", ELECTRIMACS 2008, Qubec, Canada, June 8-11 2008.

[6] R. Zanasi, F. Grossi, Differences and common aspects of POG and EMR energy-based graphical techniques, Proc. of IEEE Vehicle Power and Propulsion Conference VPPC 2011, pp.1,6

[7] R. Fuchs, Y. Hasuda, and I. James, "Dynamic performance analysis of a full toroidal IVT: A theoretical approach", International CVT and Hybrid Transmission Congress , Sacramento, USA, September 2004.

[8] R.Fuchs, T.Tamura, N. McCullough, K. Matsumoto, "The Making of the Full Toroidal Variator", JTEKT Engineering Journal English Edition No. 1006E, 2009, pp 31-36.

[9] Y.Hasuda, R.Fuchs, "Development of IVT Variator Dynamic Model", KOYO Engineering Journal English Edition No. 1060E, 2002, pp 24-28.

[10] R.Zanasi, F.Grossi "Modelling Hybrid Automotive Systems with the POG Technique", Journal of Asian Electric Vehicles, Vol. 8 (2010), Nr. 1, pp. 1379-1384

[11] R. V. Polyuga, A. van der Schaft, Structure preserving model reduction of port-Hamiltonian systems by moment matching at infinity, Automatica, Volume 46, Issue 4, April 2010, Pages 665-672, ISSN 0005-1098

[12] E. Grimme, Krylov projection methods for model reduction, Ph.D. thesis, Coordinated Science Laboratory, University of Illinois at Urbana-Champaign, 1997

[13] H. K. Khalil, Nonlinear Systems, Third Edition, Prentice Hall, 2002, ISBN 0-13-067389-7

[14] R. Zanasi, F. Grossi, N. Giuliani, "Extended and reduced POG dynamic model of an automatic corking machine for threaded plastic caps", Mechatronics, Volume 24, Issue 1, February 2014, Pages 1-11